



HAL
open science

Magnetic Pressure and Shape of Ferrofluid Seals in Cylindrical Structures

Romain Ravaud, Guy Lemarquand, Valérie Lemarquand

► **To cite this version:**

Romain Ravaud, Guy Lemarquand, Valérie Lemarquand. Magnetic Pressure and Shape of Ferrofluid Seals in Cylindrical Structures. *Journal of Applied Physics*, 2009, 106 (034911), pp.034911-1; 0.4911-9. 10.1063/1.3187560 . hal-00412386

HAL Id: hal-00412386

<https://hal.science/hal-00412386>

Submitted on 1 Sep 2009

HAL is a multi-disciplinary open access archive for the deposit and dissemination of scientific research documents, whether they are published or not. The documents may come from teaching and research institutions in France or abroad, or from public or private research centers.

L'archive ouverte pluridisciplinaire **HAL**, est destinée au dépôt et à la diffusion de documents scientifiques de niveau recherche, publiés ou non, émanant des établissements d'enseignement et de recherche français ou étrangers, des laboratoires publics ou privés.

Magnetic Pressure and Shape of Ferrofluid Seals in Cylindrical Structures

R. Ravaud, G. Lemarquand, V. Lemarquand

Abstract

This paper presents a three-dimensional analytical model for studying the shape and the pressure of ferrofluid seals submitted to intense magnetic fields produced by permanent magnet ironless structures. This three-dimensional analytical approach is based on the exact calculation of the magnetic field components created by ring permanent magnets whose polarizations are either radial or axial. We assume that the ferromagnetic particles of the ferrofluid are saturated and the static behaviour of the ferrofluid seal depends on both the magnetic field produced by the permanent magnets and the saturation magnetization of the ferrofluid particles. In our applications, ferrofluid seals are always submitted to very high magnetic fields. Consequently, the accurate knowledge of the ferrofluid seal shape as well as the magnetic pressure inside the ferrofluid seal is very useful for the design of devices using both permanent magnets and ferrofluid seals. It is emphasized here that our structures are completely ironless and thus, there are no iron-base piston for these structures. Then, this paper makes a review of the main structures using ring permanent magnets and ferrofluid seals. For each ironless structure, the shape and the pressure of the ferrofluid seals are determined. To our knowledge, this way of characterizing the static behaviour of ferrofluid seals submitted to intense magnetic fields appears for the first time in the literature. Indeed, we think that a three-dimensional analytical model is interesting for such a study because it is simple to use and has a very low computational cost.

Index Terms

ferrofluid seals, analytical approach, permanent magnets, magnetic pressure

Manuscript Revised June 29, 2009.

The authors are with the Laboratoire d'Acoustique de l'Universite du Maine UMR CNRS 6613, Avenue Olivier Messiaen, 72085 Le Mans Cedex 9, France

I. INTRODUCTION

20
21 The interest of using ferrofluid in the new technologies increases clearly with the understanding of
22 its chemical and physical properties [1]-[3]. Ferrofluids are in fact a unique class of material that have
23 been discovered in the 1960s. A ferrofluid is a stable colloidal suspension of sub-domain magnetic nano
24 particles in a liquid carrier. These magnetic particles are coated with a stabilizing dispersing agent that
25 prevents generally particle agglomeration. Such a property is very useful because in some applications
26 (as the ones presented in this paper), the magnetic fields used are very intense. Besides, it is noted that
27 we discuss the utility of using intense magnetic fields in this paper. Some industries use ferrofluids for
28 realizing airtightness seals or in audio engineering to decrease the temperature of coils in loudspeakers.
29 As this choice allows us to improve greatly these devices, a care study of the shape of a ferrofluid seal
30 must be carried out because this property is directly linked to its magnetic energy and its mechanical
31 properties. Their properties prove to be useful and efficient in various engineering areas such as damping
32 systems [4], heat transfers, motion control systems, sensors [5][6]. They also have very promising medical
33 applications [7] [8]. However, they are more commonly used in bearings and seals for rotating devices.
34 The pioneering work regarding the ferrofluid lubrication was done by Tarapov [9]. Indeed, he considered
35 a plain journal bearing lubricated by ferrofluid and submitted to a non-uniform magnetic field. Since
36 then, numerous studies in the field of ferrofluid dynamic bearings have been carried out. Both static
37 and dynamic characteristics of these bearings have been studied theoretically [10]-[17]. Moreover, recent
38 trends in the ferrofluid lubrication applications are described and discussed [18]-[24]. Ferrofluids are also
39 used in electrodynamic loudspeakers in which they fulfill several functions: they ensure the airtightness,
40 they play a heat transfer part and they work as a radial bearing. Furthermore, a ferrofluid seal can replace
41 the loudspeaker suspension and leads to a better linearity of the cone movement [25]-[29].

42

43 This paper presents a three-dimensional analytical model for studying the shape and the static pressure
44 of ferrofluid seals submitted to intense magnetic fields produced by ironless structures. We use the static
45 magnetic pressure for studying the shape of the ferrofluid seals. Our three-dimensional analytical approach
46 is based on the exact calculation of the magnetic field components created by ring permanent magnets
47 whose polarizations are either radial or axial. Moreover, the approach taken is based on the coulombian

48 model of permanent magnets. Consequently, it gives a great flexibility for the review of the different
49 structures studied in this paper.

50 In addition, it must be emphasized here that our experimental conditions in which the ferrofluid is used
51 differ from the other experiments proposed by the authors. Indeed, our applications (ironless loudspeakers,
52 bearings) require very high magnetic fields. Consequently, we think that the most important parameter
53 representing the pressure in the ferrofluid seal must be determined carefully. This term is often simplified
54 in many studies because it is difficult to determine. However, this term is not only the most important
55 parameter that must be determined carefully but this is also probably the only term that allows us to
56 study the ferrofluid seal shape. The gravitational energy or the surface tension energy do not influence a
57 ferrofluid seal shape used in these conditions. This is why we think that it is more useful to obtain an exact
58 three-dimensional analytical expression of the magnetic pressure by only considering the preponderant
59 term in the equation of equilibrium in the ferrofluid seal rather than using several simplifying terms whose
60 influence is questionable in our applications.

61 As the ferrofluid considered in this paper (Ferrotec APG05) has a saturation magnetization of at least
62 32 kA/m and the magnetic field is greater than 400 kA/m , the value of this pressure is higher than 12800
63 N/m^2 . On the other hand, the surface tension exists. But when the values of both the surface tension
64 coefficient, A , (A equals 0.0256 kg/s^2 for the used ferrofluids) and the radius of curvature are considered,
65 the effect of the surface tension can be omitted: this latter does not deform the free boundary surface.

66 II. THREE-DIMENSIONAL ANALYTICAL MODEL

67 First, we present the calculation tools to study the different configurations using one or several ring
68 permanent magnets. As the goal of this paper is to determine the shape of the ferrofluid seals for different
69 magnet configurations, the magnetic field created by the magnets must be calculated. Then, the way of
70 obtaining the seal shape is discussed.

71 It is emphasized here that we do not use a two-dimensional model for calculating the magnetic field
72 created by these arc-shaped permanent magnets because such an approach is not accurate in the enar-field
73 [30]. This is the reason why we use only a three-dimensional approach.

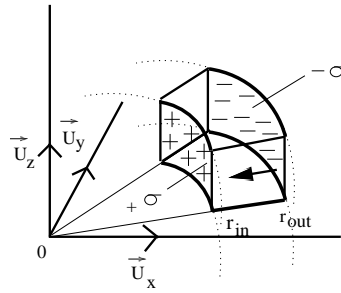


Fig. 1. Arc-shaped permanent magnet whose polarization is radial: the inner curved surface is charged with the magnetic pole surface density $+\sigma^*$ and the outer curved surface is charged with the magnetic pole surface density $-\sigma^*$, the inner radius is r_{in} , the outer one is r_{out}

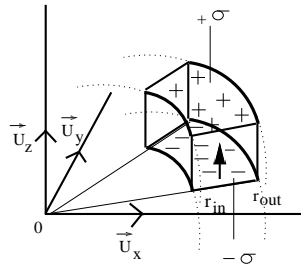


Fig. 2. Arc-shaped permanent magnet whose polarization is axial: the upper surface is charged with the magnetic pole surface density $+\sigma^*$ and the lower surface is charged with the magnetic pole surface density $-\sigma^*$, the inner radius is r_{in} , the outer one is r_{out}

74 A. Magnetic field created by the ring magnets

75 The magnetic field created by the ring magnets is determined by using the coulombian model [31][32].
 76 It is emphasized here that the authors use analytical approaches because they are more accurate than
 77 numerical methods [33]. The magnets are assumed perfect (flawless). Consequently, each permanent
 78 magnet is represented by two charged surfaces [34]. In the case of a permanent magnet whose polarization
 79 is radial, the magnetic poles are located on both curved surfaces of the ring and the magnetic pole surface
 80 density is denoted σ^* (Fig. 1). The rings are assumed radially thin enough to neglect the magnetic
 81 pole volume density related to the magnetization divergence. In the case of a permanent magnet whose
 82 polarization is axial, the magnetic pole surface density σ^* is located on the upper and lower faces of the
 83 ring (Fig. 2). The magnetic field components have been entirely determined in previous papers [35]. Since
 84 the azimuthal component equals zero because of the cylindrical symmetry [36], only two components must

85 be calculated. Therefore, the magnetic field depends on both radius r and altitude z .

86 *B. Potential energy and magnetic pressure of the ferrofluid seal*

87 The potential energy of the ferrofluid is very important parameter for the study of ferrofluid seals.
 88 Its calculation requires several assumptions, generally admitted by the authors. First, the ferromagnetic
 89 particles of the ferrofluid are assumed to be small saturated spheres which can be freely oriented in all
 90 the directions of space. Thus, all the particles of the saturated ferrofluid are aligned with the permanent
 91 magnet orienting field. In addition, when submitted to these intense magnetic fields, the ferrofluid does
 92 not modify the field created by the permanent magnets and the field created by the ferrofluid itself is
 93 omitted. Furthermore, the aggregation in chains of the ferrofluid particles is omitted [37]. It is noted that,
 94 when the device is at laboratory temperature and at rest, the aggregation phenomenon is observed. In
 95 short, the magnetic pressure is expressed as follows:

$$p_m(r, z) = \mu_0 \mathbf{M}_s \cdot \mathbf{H}(r, z) = \mu_0 M_s \sqrt{H_r(r, z)^2 + H_z(r, z)^2} \quad (1)$$

96 where both magnetic field components $H_r(r, z)$ and $H_z(r, z)$ are analytically calculated [30]. Thus, the
 97 potential energy of the ferrofluid seal, E_m , can be deducted :

$$E_m = - \int \int \int_{(\Omega)} \mathbf{H}(r, z) \cdot (\mu_0 \mathbf{M}) dV = - \int \int \int_{(\Omega)} p_m(r, z) dV \quad (2)$$

98 where (Ω) is the ferrofluid seal volume. As a remark, the magnetic pressure is given in N/m^2 and the
 99 potential energy in J . The analytical expression of the magnetic pressure depends on the number of ring
 100 permanent magnets used in the ironless structure. For example, if we consider a structure made of two
 101 ring permanent magnets radially magnetized, with opposite magnetizations, the magnetic pressure $p_m(r, z)$
 102 inside the ferrofluid seal is given by (3).

$$p_m(r, z) = \mu_0 M_s \sqrt{H_{r,2}(r, z)^2 + H_{z,2}(r, z)^2} \quad (3)$$

103 where M_s is the intensity of magnetization of a magnetic particle. The radial component $H_{r,2}(r, z)$ of
 104 the magnetic field created by the two permanent magnets is defined by (4).

$$H_{r,2}(r, z) = \frac{\sigma^*}{2\pi\mu_0} (\zeta(u_1) - \zeta(u_2)) \quad (4)$$

105 with

$$\begin{aligned} \zeta(u) = & \left(\frac{2i(1+u)\sqrt{\frac{d(-1+u)}{c+e_1+du}} (-a_1d + b_1(c+e_1)) F^* \left[i \sinh^{-1} \left[\frac{\sqrt{-c+d-e_1}}{\sqrt{c+e_1+du}} \right], \frac{c+d+e_1}{c-d+e_1} \right]}{d\sqrt{-c+d-e_1}e_1\sqrt{\frac{d(1+u)}{c+e_1+du}}\sqrt{1-u^2}} \right) \\ & + \left(\frac{2i(1+u)\sqrt{\frac{d(-1+u)}{c+e_1+du}} (b_1c - a_1d)\Pi^* \left[\frac{e_1}{c-d+e_1}, i \sinh^{-1} \left[\frac{\sqrt{-c+d+e_1}}{\sqrt{c+e_1+du}} \right], \frac{c+d+e_1}{c-d+e_1} \right]}{d\sqrt{-c+d-e_1}e_1\sqrt{\frac{d(1+u)}{c+e_1+du}}\sqrt{1-u^2}} \right) \\ & + \left(\frac{2i(1+u)\sqrt{\frac{d(-1+u)}{c+e_2+du}} (-a_2d + b_2(c+e_2)) F^* \left[i \sinh^{-1} \left[\frac{\sqrt{-c+d-e_2}}{\sqrt{c+e_2+du}} \right], \frac{c+d+e_2}{c-d+e_2} \right]}{d\sqrt{-c+d-e_2}e_2\sqrt{\frac{d(1+u)}{c+e_2+du}}\sqrt{1-u^2}} \right) \\ & + \left(\frac{2i(1+u)\sqrt{\frac{d(-1+u)}{c+e_2+du}} (b_2c - a_2d)\Pi^* \left[\frac{e_2}{c-d+e_2}, i \sinh^{-1} \left[\frac{\sqrt{-c+d+e_2}}{\sqrt{c+e_2+du}} \right], \frac{c+d+e_2}{c-d+e_2} \right]}{d\sqrt{-c+d-e_2}e_2\sqrt{\frac{d(1+u)}{c+e_2+du}}\sqrt{1-u^2}} \right) \\ & - \left(\frac{2i(1+u)\sqrt{\frac{d(-1+u)}{e_3+du}} ((a_3d - b_3e_3)) F^* \left[i \sinh^{-1} \left[\frac{\sqrt{-d-e_3}}{\sqrt{e_3+du}} \right], \frac{-d-e_3}{d+e_3} \right]}{d\sqrt{-d-e_3}(-c+e_3)\sqrt{\frac{d(1+u)}{e_3+du}}\sqrt{1-u^2}} \right) \\ & - \left(\frac{2i(1+u)\sqrt{\frac{d(-1+u)}{e_1+du}} (b_3c - a_3d)\Pi^* \left[\frac{-c+e_3}{d+e_3}, i \sinh^{-1} \left[\frac{\sqrt{-d+e_3}}{\sqrt{e_3+du}} \right], \frac{-d+e_3}{d+e_3} \right]}{d\sqrt{-d-e_3}(-c+e_3)\sqrt{\frac{d(1+u)}{e_3+du}}\sqrt{1-u^2}} \right) \\ & - \left(\frac{2i(1+u)\sqrt{\frac{d(-1+u)}{e_4+du}} (a_4d - b_4e_4) F^* \left[i \sinh^{-1} \left[\frac{\sqrt{-d-e_4}}{\sqrt{e_4+du}} \right], \frac{-d+e_4}{d+e_4} \right]}{d\sqrt{-d-e_4}(c+e_4)\sqrt{\frac{d(1+u)}{e_4+du}}\sqrt{1-u^2}} \right) \\ & - \left(\frac{2i(1+u)\sqrt{\frac{d(-1+u)}{e_4+du}} (b_4c - a_4d)\Pi^* \left[\frac{-c+e_4}{d+e_4}, i \sinh^{-1} \left[\frac{\sqrt{-d-e_4}}{\sqrt{e_4+du}} \right], \frac{-d+e_4}{d+e_4} \right]}{d\sqrt{-d-e_4}(-c+e_4)\sqrt{\frac{d(1+u)}{e_4+du}}\sqrt{1-u^2}} \right) \end{aligned} \quad (5)$$

106 The axial component of the magnetic field created by the two ring permanent magnets is given by (6).

$$\begin{aligned}
 H_{z,2}(r, z) = & \frac{\sigma^*}{\pi\mu_0} \left(-r_{in} \frac{K^* \left[-\frac{4rr_{in}}{(r-r_{in})^2+z^2} \right]}{\sqrt{(r-r_{in})^2+z^2}} + r_{in} \frac{K^* \left[-\frac{4rr_{in}}{(r-r_{in})^2+(z-h)^2} \right]}{\sqrt{(r-r_{in})^2+(z-h)^2}} \right) \\
 & - \frac{\sigma^*}{\pi\mu_0} \left(r_{in} \frac{K^* \left[\frac{4rr_{in}}{(r-r_{in})^2+z^2} \right]}{\sqrt{(r-r_{in})^2+z^2}} - r_{in} \frac{K^* \left[\frac{4rr_{in}}{(r-r_{in})^2+(z+h)^2} \right]}{\sqrt{(r-r_{in})^2+(z+h)^2}} \right)
 \end{aligned} \tag{6}$$

107 where $K^*[m]$ is given in terms of the incomplete elliptic integral of the first kind by (7)

$$K^*[m] = F^*\left[\frac{\pi}{2}, m\right] \tag{7}$$

108 $F^*[\phi, m]$ is given in terms of the elliptic integral of the first kind by (8):

$$F^*[\phi, m] = \int_{\theta=0}^{\theta=\phi} \frac{1}{\sqrt{1-m\sin(\theta)^2}} d\theta \tag{8}$$

109 $\Pi^*[n, \phi, m]$ is given in terms of the incomplete elliptic integral of the third kind by (9)

$$\Pi^*[n, \phi, m] = \int_0^\phi \frac{1}{(1-n\sin(\theta)^2)\sqrt{1-m\sin(\theta)^2}} d\theta \tag{9}$$

110 The parameters used in (5) are defined in Table II-B. Moreover, when we input (4) in Mathematica, we
 111 have to take the real part of $H_r(r, z)$ because of the noise calculus. What's more, the parameter i used
 112 in (5) is the imaginary number ($i^2 = -1$).

113 *C. Parameters used for describing the ironless structures*

114 The further calculations are presented for magnets with 1T remanent magnetization in order to normalize
 115 the results. In fact, the magnets used in the prototypes are Neodymium Iron Boron ones for which the
 116 remanent magnetization can reach 1.5T. Furthermore, the interesting regions of space are the ones where
 117 the ferrofluid goes. With these 1T normalized magnets and for the proposed configurations, the magnetic
 118 field intensity there is greater than 400 kA/m. Of course, all the field values are proportional to remanent
 119 magnetization value. Then, we use commercial ferrofluids, either from the company Ferrotec or Ferrolabs
 120 . Such ferrofluids have a saturation magnetization, M_s , smaller than 32 kA/m and a particle concentration

Parameters	
a_1	$r_{in}rz$
b_1	$-r_{in}^2z$
c	$r^2 + r_{in}^2$
d	$-2rr_{in}$
e_1	z^2
a_2	$-r_{in}r(z-h)$
b_2	$r_{in}^2(z-h)$
e_2	$(z-h)^2$
a_3	$r_{in}rz$
b_3	$-r_{in}^2z$
e_3	$r^2 + r_{in}^2 + z^2$
a_4	$r_{in}r(-z-h)$
b_4	$-r_{in}^2(-z-h)$
e_4	$r^2 + r_{in}^2 + (z+h)^2$

TABLE I
DEFINITION OF THE PARAMETERS USED IN (5)

121 below 5,5 %. It is to be noted that for bearing or loudspeaker applications, a great bearing effect is sought
 122 which requires high saturation magnetizations. Therefore, the magnetic field, H , created by the permanent
 123 magnets is far higher than the ferrofluid critical field [38]. So, the ferrofluid is totally saturated and its
 124 magnetization is denoted M_s .

125 Color plots of the magnetic pressure will be done in the further sections in order to visualize the
 126 characteristics of the studied configurations. The warmest color (red) is used for the regions of space
 127 where the magnetic pressure is the greatest and the coldest color (blue) for the ones where the magnetic
 128 pressure is the smallest. Moreover, the same color corresponds to the same value throughout this paper:
 129 the corresponding scale is given in Table II in which the magnetic pressure and the related magnetic field
 130 values are given.

131 III. SHAPE OF THE FERROFLUID SEAL IN VARIOUS MAGNETIC FIELDS

132 A. Description of the generic structure

133 Figure 3 shows the generic structure of all the devices studied. They consist of three outer stacked
 134 rings, of an inner non-magnetic piston and of ferrofluid seals. The piston is radially centered with the
 135 rings. The rings' inner radius, r_{in} , equals 25 mm and their outer radius, r_{out} , equals 28 mm. The rings

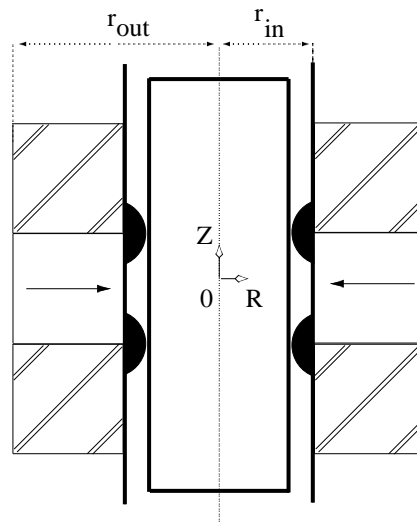


Fig. 3. Device structure: three outer rings (permanent magnet or non-magnetic) radially centered with an inner non-magnetic piston and ferrofluid seals in the air gap between the rings and the piston. $r_{in} = 25mm$, $r_{out} = 28mm$.

136 can be either made out of permanent magnet -as here the middle ring- or out of non-magnetic material
 137 -like the upper and lower rings-. For each configuration, the ferrofluid seals are located in the air gap
 138 between the piston and the rings; their number, their position as well as the magnetization direction of
 139 the ring magnets will be discussed.

140

141 For each configuration, we have also represented the radial component of the magnetic field created by
 142 the ring permanent magnets: indeed, this parameter can also be optimized by changing the ring dimensions
 143 in electric machines.

144

145 It is assumed throughout this paper that the forming shapes of ferrofluid are considered to be proportional
 146 to the magnetic pressure. Such an assumption is possible because the magnetic field produced by the ring
 147 permanent magnets is very high.

148

149 The coordinate system $(0, \vec{u}_r, \vec{u}_\theta, \vec{u}_z)$ is placed into the centre of the magnetic system in Figs 6 and
 150 7 and is axially moved off the centre in Figs 4, 5, 8, 9, 10 and 11. In addition, the radial scale of the

151 permanent magnets has been divided by 2 in these figures.

152 *B. Structures using one ring magnet*

153 The first structure considered corresponds exactly to the configuration shown in Fig.3. All the rings
154 have the same square cross-section whose side equals 3 mm. The middle ring is a radially magnetized
155 permanent magnet and the upper and lower rings are non-magnetic. The magnetic field created by the
156 magnet in the air gap is calculated at a distance in length from the rings and along the Z axis which
157 equals 0.1 mm. Moreover, its radial component H_r shown in Fig.4 is quite uniform in front of the magnet.
158 Two field gradients exist in front of the edges of the magnet. We can point out that the magnetic pressure
159 calculated in the air gap between the rings and the piston is plotted on Fig.4 as well. The ferrofluid seeks
160 the regions of both intense field gradient and high magnetic energy. The color plot shows that, for seals
161 thicker than 0.5 mm, the seal expands along the whole magnet height. A smaller amount of ferrofluid
162 would give two separate seals, but they would be too thin to have interesting mechanical properties.
163 This result is linked to the magnet square section: were the magnet higher along Z, two separate seals
164 would appear. It can be noted that this structure is the simplest one which can be used in electrodynamic
165 loudspeakers.

166 The second structure differs from the first one only in the magnetization direction which becomes
167 axial. Figure 5 shows the structure, the calculated radial field component and the corresponding magnetic
168 pressure. The radial component of the magnetic field is no longer uniform in front of the magnet; it shows
169 instead a rather large gradient all over the magnet length and the non-magnetic rings. Nevertheless, the
170 magnetic pressure deserves the same comments as in the first structure and is somewhat similar to the
171 previous one. However, it is obvious that it differs in form from one structure to the other.

172 *C. Structures using two ring magnets*

173 The structures studied here derive from the preceding ones by stacking a second permanent magnet
174 ring directly on the first one. Both ring magnets have the same dimensions and opposed magnetization
175 directions. The radial field component and the magnetic pressure are shown in Fig. 7 when the ring magnets
176 are radially magnetized and in Fig. 6 when the ring magnets are axially magnetized. The magnetic field

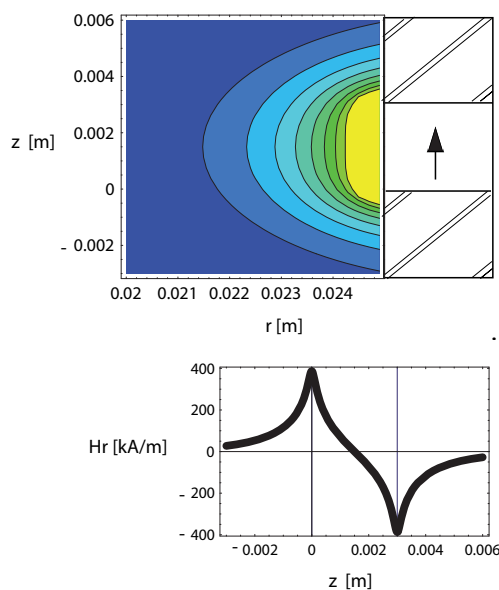


Fig. 4. Right: upper and lower non-magnetic rings, a middle ring permanent magnet axially magnetized. Left: magnetic pressure in front of the rings. Bottom: magnetic field radial component at a 0.1 mm distance from the rings, along the Z axis.

177 in both cases results from the superposition of the single magnet fields. As a consequence, each radial
 178 magnet creates a region of uniform field in front of itself and the field directions are opposite. The field
 179 intensity in each uniform region is higher than in the single magnet structure because the leakage is
 180 decreased. In effect, three field gradients exist, and the one that appears in front of the magnets' interface
 181 is twice as high as those at the edges. From the gradient point of view, Fig. 7 can be compared with
 182 Fig. 5, and the former will prove more useful because the gradient is steeper. The axial double structure
 183 creates progressive field gradients with no peculiar interest. By contrast, the radial double structure is used
 184 to design two-coil loudspeakers. The repartition of the magnetic energy density in the structure using two
 185 ring magnets does not derive from the superposition of the ones in the structures using one ring magnet.
 186 The main reason is due to the expression of the energy which depends on the square of the field. Both
 187 repartitions for radial and axial magnets seem alike at first sight, but the radial structure is in fact "more
 188 energetic" and the magnetic energy in it decreases slower at an increasing distance from the magnets.
 189 Nevertheless, the maximum energy density is in front of the magnets' interface and the ferrofluid seal
 190 will be located there. We can point out that the axial length of the seal in structures using one magnet is

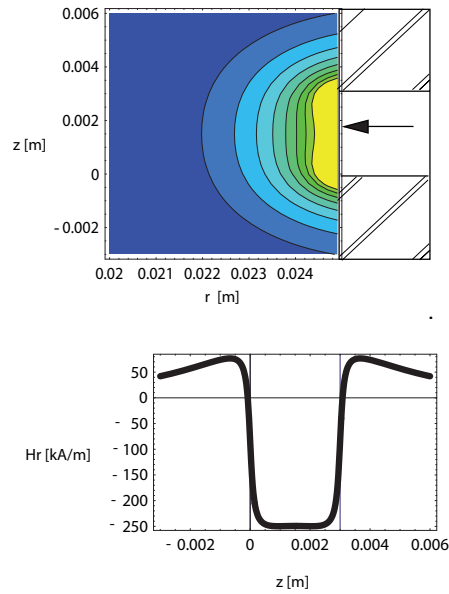


Fig. 5. Right: upper and lower non-magnetic rings, a middle ring permanent magnet radially magnetized. Left: magnetic pressure in front of the rings. Bottom: magnetic field radial component at a 0.1 mm distance from the rings, along the Z axis.

191 smaller than the one in structures using two ring magnets. Furthermore, its energy density is approximately
 192 doubled for the radial magnets.

193 *D. Structures using three ring magnets*

194 All the structures considered now consist of three stacked ring permanent magnets whose magnetization
 195 directions undergo a 90 degrees rotation from one magnet to the neighboring one. Such configurations
 196 with a magnetization progressive rotation are related to Halbach cylinders [39] and to their applications in
 197 the design of electrical motors [40] or of passive magnetic bearings [41]. Contrary to electrical machines,
 198 the presented structures do not have a periodical magnet pattern.

199 Figure 8 shows the field radial component and the magnetic pressure for an assembly of a radially
 200 magnetized middle ring and two axially magnetized upper and lower rings. Moreover, the axial magnets
 201 have opposed magnetization directions. In Fig. 9, the middle ring is axially magnetized, both other rings

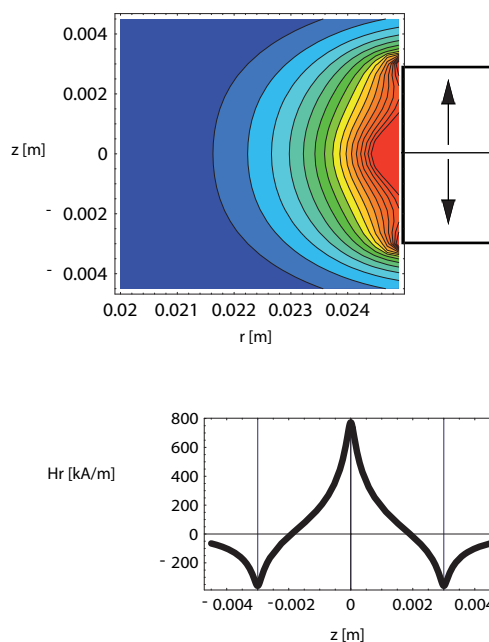


Fig. 6. Right: Two ring permanent magnets with opposed axial magnetization. Left: magnetic pressure in front of the rings. Bottom: magnetic field radial component at a 0.1 mm distance from the rings, along the Z axis.

202 are radially magnetized with opposed directions.

203 The energy density color plots show that two ferrofluid seals form in front of the magnets' interfaces
 204 and that those seals have a great magnetic energy. Consequently, they own good mechanical properties
 205 (great radial stiffness for example). The seals are rather similar in both structures. However, the magnetic
 206 field radial component shown in Fig. 8 is fairly uniform in the area in front of the middle magnet while it
 207 varies with no particularly interesting properties in Fig. 9. Therefore, the structure with the radial middle
 208 magnet is the useful one, especially for the loudspeaker design, and the field uniformity zone may be
 209 optimized.

210 The axial height of the middle magnet can be varied regarding the axial height of the upper and lower
 211 magnets. For example, the middle magnet is twice as high as each other magnet in Fig. 10 and half as
 212 small in Fig. 11. As a result, the length of the field uniformity area follows closely the middle magnet
 213 height. If the latter increases, the former increases too. We can say that the ratio middle of the magnet

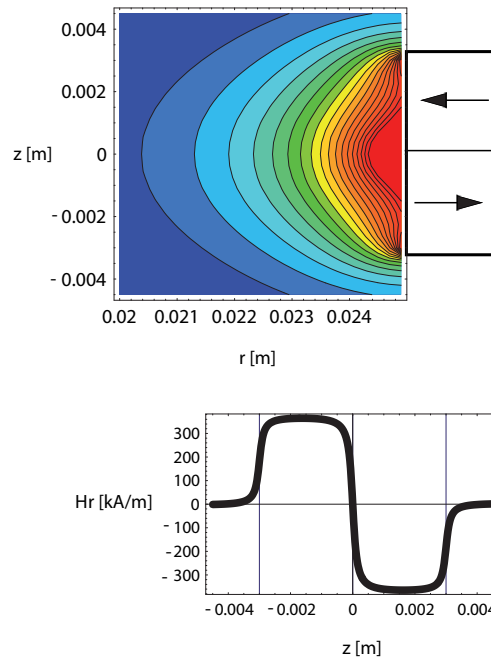


Fig. 7. Right: Two ring permanent magnets with opposed radial magnetization. Left: magnetic pressure in front of the rings. Bottom: magnetic field radial component at a 0.1 mm distance from the rings, along the Z axis.

214 height over the upper and lower magnet height is important as well. Indeed, if it increases, the field
 215 uniformity region grows but the field intensity decreases, and inversely. It also influences the repartition
 216 of the magnetic pressure. Indeed, when the upper and lower magnets become too small, the ferrofluid
 217 can expand over their whole axial length and the seals can become fairly voluminous, depending on the
 218 ferrofluid available quantity. The field gradients are steep and the seal magnetic energy is quite high.
 219 Consequently, the seals are well-fixed to the structure and have high mechanical performances. Inversely,
 220 when the middle magnet becomes too small, both seals gather to form a single one which expands over
 221 the whole height of the middle magnet. The energy in the seal is still high for radial thickness smaller
 222 than the ones presented in the previous case.

223 *E. Discussion*

224 So far, different magnet assemblies have been presented. Each assembly creates magnetic fields and
 225 magnetic field gradients so as to trap and fix ferrofluid to make seals. Their characteristics will be discussed

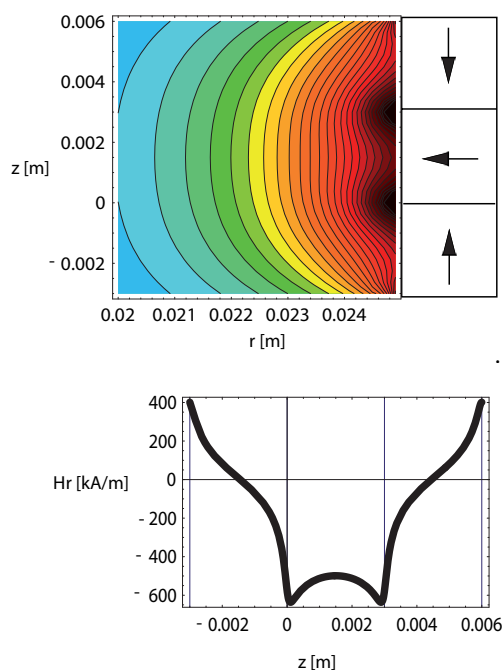


Fig. 8. Right: axially magnetized upper and lower rings, radially magnetized middle ring. Left: magnetic pressure in front of the rings. Bottom: magnetic field radial component at a 0.1 mm distance from the rings, along the Z axis.

226 and compared now.

227 The structures considered are either very simple or more complex. The complexity can be characterized
 228 by the number of separate parts necessary to build devices. We can say that from this point of view, the
 229 single magnet structures are the simplest ones. The complexity also lies in the magnets' magnetization
 230 direction. Indeed, an axial magnetization is easy to achieve for ring magnets whereas a radial one is
 231 technically more difficult. Thereby, ring magnets whose polarization is radial are more expensive than
 232 the ones whose polarization is axial. Nevertheless, some magnet manufacturers begin to deal with radial
 233 magnetization and to sell such products.

234 The utility of a structure depends on the intended applications. For example, a device can be designed
 235 solely to make ferrofluid seals with good mechanical properties. It can also be designed to create a radial
 236 magnetic field or to enable a ferrofluid seal to form as it is required in loudspeakers.

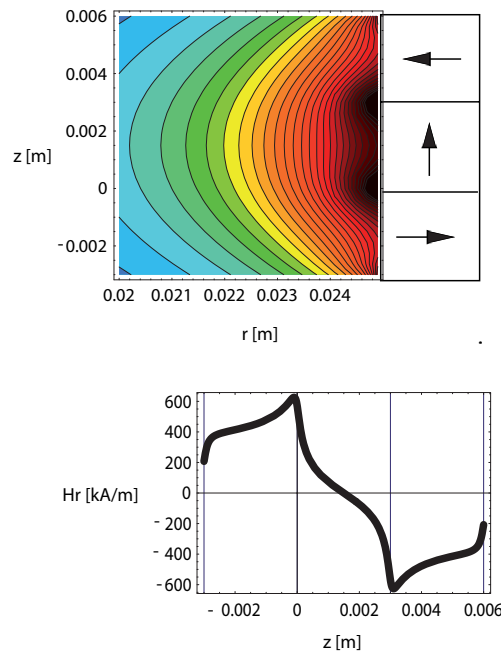


Fig. 9. Right: radially magnetized upper and lower rings, axially magnetized middle ring. Left: magnetic pressure in front of the rings. Bottom: magnetic field radial component at a 0.1 mm distance from the rings, along the Z axis.

237 A high magnetic field gradient and a high magnetic pressure are required to achieve robust seals. From
 238 the preceding sections, we deduce that multi-magnet structures are more efficient than single magnet
 239 structures in creating high field gradients. Furthermore, the magnetic pressure is higher in the air gap near
 240 the magnets.

241 It can be emphasized here that the shape of the ferrofluid seal in the device depends on both the
 242 magnetic pressure and the ferrofluid volume. It can be noted that this latter one is related to the air
 243 gap size. The air gap exists because the inner part has to move, in rotation or in translation, inside the
 244 outer part without rubbing against it. The air gap size depends on mechanical considerations, such as the
 245 practical machining and the related possible tolerances. The color plots show clearly that the theoretical
 246 size of the air gap which allows an efficient ferrofluid seal depends on the magnetic structure dimensions.

247 For example, the structures shown in Fig. 11 or in Fig. 8 lead to seals thinner than the ones shown in
 248 Fig. 7 because the region of high magnetic pressure is radially thinner.

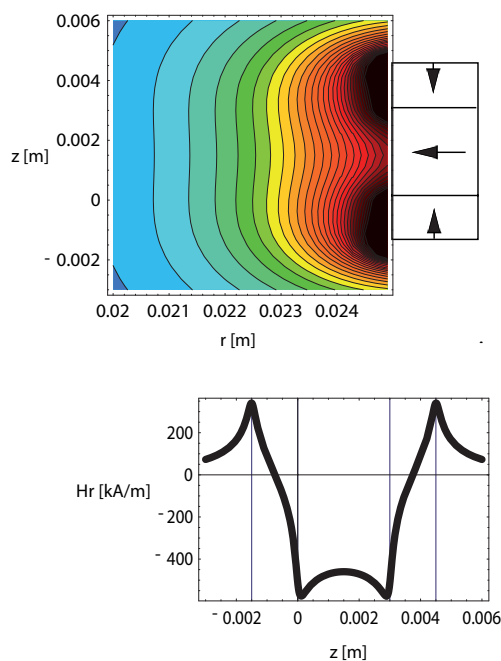


Fig. 10. Right: axially magnetized upper and lower rings, radially magnetized middle ring, each axial magnet is half as small as the radial one. Left: magnetic pressure in front of the rings. Bottom: magnetic field radial component at a 0.1 mm distance from the rings, along the Z axis.

249 Ferrofluid seals are robust when their capacity is high; this means that they can resist to quite high
 250 axial pressures because they exert themselves an opposing force. We can say that this force is related to
 251 the energy variation of the ferrofluid seal. The higher the energy varies with the axial displacement, the
 252 more important the force is.

253 Moreover, a great force is attained with thin seals whose energy is high and varies extremely with axial
 254 displacements. Therefore, the smaller the air gap is, the more favorable the mechanical structure to build
 255 ferrofluid seals is.

256 The color plots can help optimizing both the number and the shape of ferrofluid seals for given ferrofluid
 257 volumes.

258 For example, the plots shown in Figs. 10 and 11 point out that two seals appear in these three magnet
 259 structures for a small volume of ferrofluid. Moreover, they show that the increase in the ferrofluid volume
 260 results in the growth of the seals which eventually join and can form a single big one.

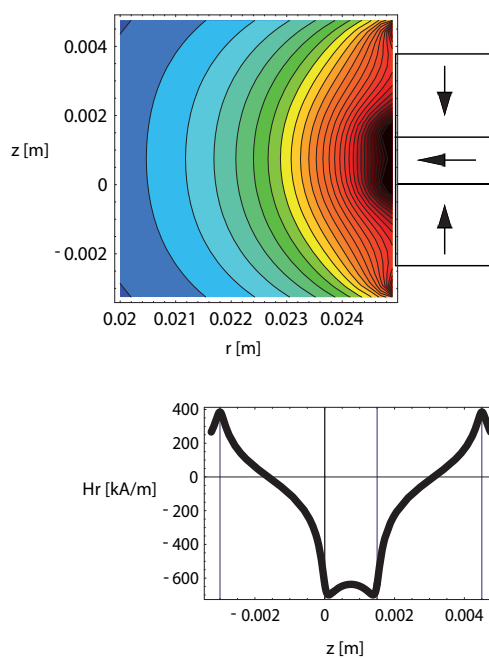


Fig. 11. Right: axially magnetized upper and lower rings, radially magnetized middle ring, each axial magnet is twice as high as the radial one. Left: magnetic pressure in front of the rings. Bottom: magnetic field radial component at a 0.1 mm distance from the rings, along the Z axis.

261 The color plots can also be considered as tools to determine the adequate quantity of ferrofluid which
 262 will confer the intended mechanical properties on the seals. Furthermore, this study shows that some
 263 structures have greater performances than others for given magnet and ferrofluid volumes.

264 The requirements for the loudspeaker applications are different. Indeed, the magnetic structure is
 265 expected to fulfill several purposes, namely the creation of a radial uniform magnetic field as well as
 266 the creation of field gradients. Besides, a loudspeaker coil moves thanks to the magnetic field. The
 267 linearity performances are related to the field uniformity and the efficiency is proportional to the field
 268 level. Furthermore, the ferrofluid seal is used to ensure the airtightness, to transfer the heat from the
 269 moving part to the steady one, to work as a radial bearing and to replace the loudspeaker suspension.
 270 Thereby, it contributes to the improvement of the loudspeaker linearity. The air gaps in loudspeakers are
 271 generally 0.1 to 0.5 mm wide: this explains why the presented magnetic field calculations have been
 272 carried out along a path at a distance in length which equals 0.1 mm from the ring magnets. Thinner

273 air gaps would be more advantageous for ferrofluid seals but are not technically possible because of the
274 machining tolerances or the recognition of the moving part thermal dilation. Therefore, the structures
275 shown in Figs. 3, 7 and 10 are the ones that are the more useful for loudspeakers. The three magnet
276 structures are the more complex, but they offer the possibility of a multi-criteria optimization. We can
277 say that this optimization is enabled and simplified by the analytical formulations of both the magnetic
278 field and the magnetic energy density. Eventually, such structures show very good performances.

279 IV. CONCLUSION

280 This paper has presented a three-dimensional analytical model for studying the shape of the static
281 pressure of ferrofluid seals subject to intense magnetic fields produced by permanent magnet ironless
282 structures. Our analytical approach has been applied to well-known structures composed of one, two or
283 three stacked ring permanent magnets whose polarization is either radial or axial. Our analytical approach
284 allows us to predict easily the shape and the pressure of ferrofluid seals. Then, we have discussed the
285 interest of using simple or complex structures with ferrofluid seals. The single magnet structures are the
286 simplest ones but the less efficient. The use of several magnets enhances both magnetic and mechanical
287 properties: when the created magnetic field is doubled, the magnetic energy is quadrupled. Furthermore,
288 three magnet structures enable to create one or two seals which have a high energy. The structures can
289 also create a high uniform magnetic field over defined regions as well as efficient ferrofluid seals: this
290 is useful for loudspeaker applications. The results obtained can be used for the design of cylindrical
291 structures using both ring permanent magnets and ferrofluid seals.

292 REFERENCES

- 293 [1] H. S. Choi, Y. S. Kim, K. T. Kim, and I. H. Park, "Simulation of hydrostatical equilibrium of ferrofluid subject to magneto-static
294 field," *IEEE Trans. Magn.*, vol. 44, no. 6, pp. 818–821, 2008.
- 295 [2] K. Raj, V. Moskowitz, and R. Casciari, "Advances in ferrofluid in ferrofluid technology," *Journal of Magnetism and Magnetic
296 Materials*, vol. 149, pp. 174–180, 1995.
- 297 [3] Y. L. Raikher, V. I. Stepanov, J. C. Bacri, and R. Perzynski, "Orientational dynamics in magnetic fluids under strong coupling
298 of external and internal relaxations," *Journal of Magnetism and Magnetic Materials*, vol. 289, pp. 222–225, 2005.
- 299 [4] J. Bajkowski, J. Nachman, M. Shillor, and M. Sofonea, "A model for a magnetorheological damper," *Mathematical and
300 computer modelling*, vol. 48, pp. 56–68, 2008.

- 301 [5] R. E. Rosensweig, *Ferrohydrodynamics*. Dover, 1997.
- 302 [6] O. Doutres, N. Dauchez, J. M. Genevaux, and G. Lemarquand, "On the use of a loudspeaker for measuring the viscoelastic
303 properties of sound absorbing materials," *Journal of the Acoustical Society of America Express Letters*, vol. 124, no. 6,
304 pp. EL335–EL340, 2008.
- 305 [7] X. Li, K. Yao, and Z. Liu, "Cfd study on the magnetic fluid delivering in the vessel in high-gradient magnetic fields," *Journal*
306 *of Magnetism and Magnetic Materials*, vol. 320, pp. 1753–1758, 2008.
- 307 [8] G. S. Park and K. Seo, "New design of the magnetic fluid linear pump to reduce the discontinuities of the pumping forces,"
308 *IEEE Trans. Magn.*, vol. 40, pp. 916–919, 2004.
- 309 [9] I. Tarapov, "Movement of a magnetizable fluid in lubricating layer of a cylindrical bearing," *Magneto hydrodynamics*, vol. 8,
310 no. 4, pp. 444–448, 1972.
- 311 [10] J. Walker and J. Backmaster, "Ferrohydrodynamics thrust bearings," *Int. J. Eng. Sci.*, vol. 17, pp. 1171–1182, 1979.
- 312 [11] N. Tiperi, "Overall characteristics of bearings lubricated ferrofluids," *ASME J. Lubr. Technol.*, vol. 105, pp. 466–475, 1983.
- 313 [12] S. Miyake and S. Takahashi, "Sliding bearing lubricated with ferromagnetic fluid," *ASLE Trans.*, vol. 28, pp. 461–466, 1985.
- 314 [13] H. Chang, C. Chi, and P. Zhao, "A theoretical and experimental study of ferrofluid lubricated four-pocket journal bearing,"
315 *Journal of Magnetism and Magnetic Materials*, vol. 65, pp. 372–374, 1987.
- 316 [14] Y. Zhang, "Static characteristics of magnetized journal bearing lubricated with ferrofluids," *ASME J. Tribol.*, vol. 113, pp. 533–
317 538, 1991.
- 318 [15] T. Osman, G. Nada, and Z. Safar, "Static and dynamic characteristics of magnetized journal bearings lubricated with ferrofluid,"
319 *Tribology International*, vol. 34, pp. 369–380, 2001.
- 320 [16] R. C. Shah and M. Bhat, "Anisotropic permeable porous facing and slip velocity squeeze film in axially undefined journal
321 bearing with ferrofluid lubricant," *Journal of Magnetism and Magnetic Materials*, vol. 279, pp. 224–230, 2004.
- 322 [17] F. Cunha and H. Couto, "A new boundary integral formulation to describe three-dimensional motions of interfaces between
323 magnetic fluids," *Applied mathematics and computation*, vol. 199, pp. 70–83, 2008.
- 324 [18] R. C. Shah and M. Bhat, "Ferrofluid squeeze film in a long bearing," *Tribology International*, vol. 37, pp. 441–446, 2004.
- 325 [19] S. Chen, Q. Zhang, H. Chong, T. Komatsu, and C. Kang, "Some design and prototyping issues on a 20 krpm hdd spindle
326 motor with a ferro-fluid bearing system," *IEEE Trans. Magn.*, vol. 37, no. 2, pp. 805–809, 2001.
- 327 [20] Q. Zhang, S. Chen, S. Winoto, and E. Ong, "Design of high-speed magnetic fluid bearing spindle motor," *IEEE Trans. Magn.*,
328 vol. 37, no. 4, pp. 2647–2650, 2001.
- 329 [21] P. Kuzhir, "Free boundary of lubricant film in ferrofluid journal bearings," *Tribology International*, vol. 41, pp. 256–268, 2008.
- 330 [22] M. Miwa, H. Harita, T. Nishigami, R. Kaneko, and H. Unozawa, "Frequency characteristics of stiffness and damping effect
331 of a ferrofluid bearing," *Tribology Letter*, vol. 15, no. 2, pp. 97–105, 2003.
- 332 [23] W. Ochonski, "The attraction of ferrofluid bearings," *Mach. Des.*, vol. 77, no. 21, pp. 96–102, 2005.
- 333 [24] Z. Meng and Z. Jibin, "An analysis on the magnetic fluid seal capacity," *Journal of Magnetism and Magnetic Materials*,
334 vol. 303, pp. e428–e431, 2006.
- 335 [25] R. E. Rosensweig, Y. Hirota, S. Tsuda, and K. Raj, "Study of audio speakers containing ferrofluid," *J. Phys. : Condens. Matter*,
336 vol. 20, 2008.
- 337 [26] G. Lemarquand, "Ironless loudspeakers," *IEEE Trans. Magn.*, vol. 43, no. 8, pp. 3371–3374, 2007.

- 338 [27] R. Ravaud and G. Lemarquand, "Modelling an ironless loudspeaker by using three-dimensional analytical approaches," *Progress*
339 *in Electromagnetics Research, PIER 91*, pp. 53–68, 2009.
- 340 [28] R. Ravaud, G. Lemarquand, V. Lemarquand, and C. Depollier, "Ironless loudspeakers with ferrofluid seals," *Archives of*
341 *Acoustics*, vol. 33, no. 4, pp. 3–10, 2008.
- 342 [29] R. Ravaud and G. Lemarquand, "Mechanical properties of a ferrofluid seal: three-dimensional analytical study based on the
343 coulombian model," *Progress in Electromagnetics research B*, vol. 13, pp. 385–407, 2009.
- 344 [30] R. Ravaud, G. Lemarquand, V. Lemarquand, and C. Depollier, "Analytical calculation of the magnetic field created by
345 permanent-magnet rings," *IEEE Trans. Magn.*, vol. 44, no. 8, pp. 1982–1989, 2008.
- 346 [31] S. I. Babic and C. Akyel, "Improvement in the analytical calculation of the magnetic field produced by permanent magnet
347 rings," *Progress in Electromagnetics Research C*, vol. 5, pp. 71–82, 2008.
- 348 [32] R. Ravaud, G. Lemarquand, V. Lemarquand, and C. Depollier, "Magnetic field produced by a tile permanent magnet whose
349 polarization is both uniform and tangential," *Progress in Electromagnetics Research B*, vol. 13, pp. 1–20, 2009.
- 350 [33] C. Akyel, S. I. Babic, and M. M. Mahmoudi, "Mutual inductance calculation for non-coaxial circular air coils with parallel
351 axes," *Progress in Electromagnetics Research*, vol. PIER 91, pp. 287–301, 2009.
- 352 [34] R. Ravaud and G. Lemarquand, "Analytical expression of the magnetic field created by tile permanent magnets tangentially
353 magnetized and radial currents in massive disks," *Progress in Electromagnetics Research B*, vol. 13, pp. 309–328, 2009.
- 354 [35] R. Ravaud, G. Lemarquand, V. Lemarquand, and C. Depollier, "Discussion about the analytical calculation of the magnetic
355 field created by permanent magnets.," *Progress in Electromagnetics Research B*, vol. 11, pp. 281–297, 2009.
- 356 [36] R. Ravaud, G. Lemarquand, V. Lemarquand, and C. Depollier, "The three exact components of the magnetic field created by
357 a radially magnetized tile permanent magnet.," *Progress in Electromagnetics Research, PIER 88*, pp. 307–319, 2008.
- 358 [37] A. Ivanov, S. Kantorovich, V. Mendelev, and E. Pyanzina, "Ferrofluid aggregation in chains under the influence of a magnetic
359 field," *Journal of Magnetism and Magnetic Materials*, vol. 300, pp. e206–e209, 2006.
- 360 [38] G. Matthies and U. Tobiska, "Numerical simulation of normal-field instability in the static and dynamic case," *Journal of*
361 *Magnetism and Magnetic Materials*, vol. 289, pp. 436–439, 2005.
- 362 [39] K. Halbach, "Design of permanent multiple magnets with oriented rec material," *Nucl. Inst. Meth.*, vol. 169, pp. 1–10, 1980.
- 363 [40] M. Marinescu and N. Marinescu, "Compensation of anisotropy effects in flux-confining permanent-magnet structures," *IEEE*
364 *Trans. Magn.*, vol. 25, no. 5, pp. 3899–3901, 1989.
- 365 [41] J. P. Yonnet, "Permanent magnet bearings and couplings," *IEEE Trans. Magn.*, vol. 17, no. 1, pp. 1169–1173, 1981.

$H[kA/m]$	$p_m (N.m^{-2})$
630	25200
610	24300
590	23400
570	22800
550	22000
530	21200
510	20400
490	19600
470	18800
450	18000
430	17200
410	16400
390	15600
370	14800
350	14000
330	13200
310	12400
290	11600
270	10800
250	10000
230	9200
210	8400
190	7600
170	6800
150	6000
130	5200
110	4400
90	3600
70	2800
50	2000

TABLE II

H , MODULUS OF THE MAGNETIC FIELD (kA/m); p_m , MAGNETIC PRESSURE ($N.m^{-2}$); $M_s = 32kA/m$